# Identification and Characterization of a Small Molecule Inhibitor of Fatty Acid Binding Proteins

**ARTICLE** *in* JOURNAL OF MEDICINAL CHEMISTRY · SEPTEMBER 2009

Impact Factor: 5.45 · DOI: 10.1021/jm900720m · Source: PubMed

Published in final edited form as:
*J Med Chem*. 2009 October 8; 52(19): 6024–6031. doi:10.1021/jm900720m.

# Identification and Characterization of a Small Molecule Inhibitor of Fatty Acid Binding Proteins†

**Ann V. Hertzel**[1], **Kristina Hellberg**[1], **Joseph M. Reynolds**[2], **Andrew C. Kruse**[1], **Brittany E. Juhlmann**[1], **Anne J. Smith**[1], **Mark A. Sanders**[3], **Douglas H. Ohlendorf**[1], **Jill Suttles**[2], and **David A. Bernlohr**[1,*]

[1]Departments of Biochemistry, Molecular Biology, and Biophysics, University of Minnesota, Minneapolis, MN 55455

[2]Department of Microbiology and Immunology, University of Louisville School of Medicine, Louisville, KY 40292

[3]Imaging Center, University of Minnesota, Minneapolis, MN 55455

## Abstract

Molecular disruption of the lipid carrier AFABP/aP2 in mice results in improved insulin sensitivity and protection from atherosclerosis. Since small molecule inhibitors may be efficacious in defining the mechanism(s) of AFABP/aP2 action, a chemical library was screened and identified **1** (HTS01037) as a pharmacologic ligand capable of displacing the fluorophore 1-anilinonaphthalene 8-sulfonic acid from the lipid binding cavity. The X-ray crystal structure of **1** bound to AFABP/aP2 revealed that the ligand binds at a structurally similar position to a long-chain fatty acid. Similar to AFABP/aP2 knockout mice, **1** inhibits lipolysis in 3T3-L1 adipocytes and reduces LPS-stimulated inflammation in cultured macrophages. **1** acts as an antagonist of the protein-protein interaction between AFABP/aP2 and hormone sensitive lipase but does not activate PPARγ in macrophage or CV-1 cells. These results identify **1** as an inhibitor of fatty acid binding and a competitive antagonist of protein-protein interactions mediated by AFABP/aP2.

## Introduction

Fatty acid binding proteins (FABPs) are small molecular weight proteins containing a central cavity that bind a long chain fatty acids or other hydrophobic ligands[1]. Each FABP gene exhibits a unique expression pattern and all cells that carry out extensive lipid metabolism express one or more FABP(s). The primary sequences of the nine family members vary significantly (as little as 20% amino acid identity), however their tertiary structures are virtually superimposable. FABPs are abundantly expressed and function to promote intracellular fatty acid solubilization, trafficking and metabolism[1, 2]. The adipocyte member of the FABP family (AFABP, also known as aP2) is expressed in both adipocytes and macrophages, two cell types that play major roles in overall whole body metabolic homeostasis[3].

To delineate the specific physiological function(s) of AFABP/aP2 in adipose tissue, knockout mice have been generated and although these animals develop obesity in response to a high fat diet, they exhibited significant resistance to a cluster of pathologies including decreased insulin

†X-ray coordinates have been deposited in the protein data bank for AFABP/aP2 complexed with **1** (PBD ID 3HK1).

*Author to whom correspondence should be addressed: Dr. David A. Bernlohr, Department of Biochemistry, Molecular Biology, and Biophysics, University of Minnesota, 6-155 Jackson Hall, 321 Church St. SE, Minneapolis, MN 55455, Tel: 612-624-2712, Fax: 612-625-2163, bernl001@umn.edu.

sensitivity, asthma and atherogenesis[4-6]. As shown by both in situ and in vivo technologies, adipocyte lipolysis was reduced under both basal and stimulated conditions[7-9]. Furthermore, inflammatory cytokine production in response to LPS was reduced in macrophages from AFABP/aP2 knockout mice[10].

All members of the FABP family share a similar structure derived from two α-helices and ten anti-parallel β-strands folded into two β-sheets[11-13]. The overall protein fold is typically called a β-barrel or β-clam and importantly for function, forms an internal water-filled ligand-binding cavity. Although this cavity binds hydrophobic ligands, it contains a hydrogen bond network involving the side chains and main chain atoms linked through numerous disordered and ordered water molecules. The comparative ligand binding properties of many FABPs for various fatty acids has been defined by Kleinfeld and colleagues and although there are subtle isoform-specific differences, the proteins as a class bind a variety of long chain fatty acids[14]. Molecular disruption of AFABP/aP2 may increase the bioavailability of fatty acids for metabolism by alternate pathways: a process that may underlie the broad metabolic phenotype of the knockout mice.

Recent work has demonstrated that beyond fatty acid solubilization and trafficking, AFABP/aP2 physically associates with at least three different intracellular proteins in a fatty acid dependent manner suggesting that the protein may serve a regulatory role as a lipid sensor. Work by Jenkins-Kruchten et al.[15] and subsequently by Smith et al.[16] have shown that AFABP/aP2 physically associates with the adipocyte hormone sensitive lipase (HSL) in a reaction that requires a fatty acid bound to the FABP. Such an interaction is likely to be regulatory and would feedback inhibit lipolysis. More recently, Thompson et al.[17] have shown that AFABP/aP2 interacts with Jak2 in a fatty acid dependent manner and affects IL-6 dependent signaling in macrophages. In addition, work from the Spener and Noy laboratories has shown that AFABP/aP2 interacts with the nuclear hormone receptor peroxisome proliferator activated receptor γ[18, 19]. The results of all protein-protein interaction studies suggest that AFABP/aP2 may act as a lipid sensor and affect adipocyte metabolism, signaling and gene expression via a series of targeted interactions.

To evaluate the molecular mechanism of AFABP/aP2 function in adipocytes and macrophages, we reasoned that small molecule inhibitors of AFABP/aP2 may be efficacious tools. To that end, we report herein the identification and analysis of a small molecule inhibitor of AFABP/aP2 that not only blocks fatty acid binding but also antagonizes physical interaction with HSL. Such a molecule reproduces many of the phenotypes of the AFABP/aP2 null mouse with regard to lipid metabolism in fat cells and inflammation in macrophages and may be useful in delineating FABP function.

## Results

### Identification of a small molecule ligand of AFABP/aP2

To evaluate the various models of AFABP/aP2 function, knockout mice have been generated and their phenotype characterized[4-6]. AFABP/aP2 null mice exhibit decreased rates of basal and stimulated lipolysis, as well as reduced lipogenesis[7-9, 20]. Although still prone to diet-induced obesity, the knockout mice maintain an improved metabolic state, including increased insulin sensitivity, increased insulin secretion and resistance to atherosclerosis and asthma[4-6].

To identify a small molecule that could antagonize the function of AFABP/aP2 and potentially mimic the AFABP/aP2 null phenotype, we took advantage of a fluorescent displacement assay[21] allowing high throughput screening of a small molecule library. Of the approximately 5,000 compounds, seven positive hits were obtained in the first round, of which five were

reproduced in a second round of screening. Four of these reproducibly displaced the fluorescent probe. One molecule was selected for further study, **1** (HTS01037), which functioned as a high affinity ligand of AFABP/aP2 (Figure 1) with an apparent $K_i$ of 0.67 ± 0.18 μM (Table 1). To test whether **1** is specific for AFABP/aP2 or would bind to other members of the FABP family, liver, intestinal, heart muscle and epithelial FABPs were also tested for binding. The results show that **1** binds to other FABPs, although with somewhat reduced affinities indicating that the small molecule is somewhat selective for AFABP/aP2, but at higher concentrations is a pan-specific FABP inhibitor (Table 1).

## Determination of the X-ray crystal structure of 1 complexed to AFABP/aP2

Various X-ray structures of FABP family members have been solved that upon comparison reveal a conserved three-dimensional fold of a β-barrel or β-clam shape. For AFABP/aP2, both apo and holo structures have been determined[22-27]. Using molecular replacement methods we determined the structure of AFABP/aP2 with **1** bound in the ligand cavity at 1.7Å resolution (Figure 2A).

Not surprisingly, the crystal structure of AFABP/aP2 with **1** shares the same conserved fold with the previously solved crystal structures. It consists of 10 anti-parallel β-strands folded into two β-sheets, which form a β-barrel with an internal ligand-binding cavity. A helix-turn-helix motif serves to close the main opening to the β-barrel from the surroundings. The volume of the ligand-binding cavity is large (1099 $Å^3$ as estimated with CASTp with a probe radius of 1.4 Å[28]), and contains both ordered and disordered water molecules. Even though there is an increase in the number of water molecules in the structure of AFABP~aP2 with **1** compared to the apo form (PDB ID 1LIB) and AFABP~aP2 with bound oleic acid (PDB ID 1LID), the positions of many ordered water molecules are conserved in the ligand-binding cavity between the structures.

The presence and positioning of **1** in the ligand-binding cavity is unambiguous due to the tight binding of the ligand and the high resolution of the data (Figure 3B). **1** adopts a planar conformation and binds, as do fatty acids, in the ligand-binding cavity with its carboxyl group coordinated by hydrogen bonds to R126 and Y128 (Figure 3A). In the structure of AFABP~aP2 complexed with oleic acid, the carboxyl group is also coordinated through hydrogen bonds to R106 via a bridging water molecule. This is not the situation in the **1** structure where the corresponding water molecule is shifted and positioned too far away from the carboxyl group to bridge it to R106.

Besides interactions between the carboxylate and the side chains of R126 and Y128, structural examination of **1** reveals a number of additional interactions with residues of the cavity and water molecules. The carbonyl oxygen of the ester bond of **1** interacts through a hydrogen bonding with a water molecule located 3.04 Å away. This water molecule in turn is involved in the large water network inside the ligand-binding cavity of the protein. In addition, the distance between the ester carbonyl group and the nitrogen atom of molecule **1** is less than 3 Å suggesting that an intramolecular hydrogen interaction may be formed between these two atoms. The amide nitrogen can also form a hydrogen bond (3.34 Å) to the same water molecule as does the ester carbonyl oxygen. Secondly, **1** contains two thiofuran rings referred to as proximal and distal, relative to the carboxylate function. The proximal thiofuran ring of **1** is positioned near the ether oxygen of the ester group potentially forming an H-bond. The sulfur atom of the distal thiofuran of **1** is within H-bonding distance with the main chain carbonyl of A75. Despite the extensive interaction network between 1 and cavity amino acids and water molecules, no major conformational shifts in the AFABP/aP2 structure are observed upon binding of the ligand, which is consistent with previously reported structures of AFABP~aP2 in complex with different ligands. However, three regions deserve further examination: the side chain of F57, the charge quartet, and the A36-K37 peptide flip.

F57 is a residue positioned in a loop region lining the opening to the ligand-binding cavity close to the helix-turn-helix domain. This residue undergoes a large conformational shift from a closed to an open form upon binding of certain ligands. It has been suggested that F57 can adopt different orientations in order to allow entry or exit of the ligand from the cavity[29, 30]. In the crystal structure of AFABP̃aP2 with **1**, F57 exists in an open conformation, an orientation also observed in the AFABP̃aP2 structure with bound oleic acid while the apo form and AFABP̃aP2 with linoleic acid (PDB ID 2Q9S) exist in the closed conformation (Figure 2B).

The helix-turn-helix motif of AFABP̃aP2 has been implicated in the interactions with HSL and Jak2. Four charged residues located in this motif, referred to as the charge quartet, form two ion pairs, D17-R30 and D18-K21, and are required for HSL-interaction[31]. Compared to the apo form of AFABP̃aP2, the distance between the D17 and R30 ion pair is slightly decreased in the crystal structure of AFABP̃aP2 with bound **1**, from 3.26 Å to 2.95 Å, respectively. For the D18-K21 ion pair the distance is 4.01 Å in the apo structure and increases to 4.78 Å in the structure with **1** (Figure 2C).

In some of the previously reported structures of AFABP̃aP2, a rotation of the peptide bond between A36 and K37 has been observed compared to the apo form of the protein. Not all ligands, however, induce this peptide flip, such as linoleic acid and troglitazone (PDB ID 2QM9) bound in the ligand-binding cavity. The peptide flip is present in the structure of AFABP̃aP2 with **1** (Figure 2D).

We modeled the **1** molecule from AFABP/aP2 into liver FABP using Modeller 9.5[32] (data not shown). Upon analysis, it is not clear what molecular determinants result in **1** binding with higher affinity to AFABP/aP2 than to LFABP. The carboxyl group of **1** is coordinated through R122 and N111 in LFABP instead of R126 and Y128 in AFABP/aP2 and there is no obviously identifiable region that would sterically or electrostatically affect **1** association with LFABP.

### 1 inhibits the interaction of AFABP̃aP2 with HSL

Previous studies have indicated that AFABP/aP2 physically interacts with HSL[33-35] and that this interaction requires a ligand bound to AFABP/aP2[15, 16]. To determine if **1** mimicked the lipid bound form of AFABP/aP2, we tested whether it would positively or negatively influence the interaction with HSL, as measured via FRET. This evaluation was conducted under basal as well as forskolin stimulation and a DIC image included to verify the dispersal of the large lipid droplet upon forskolin treatment (Figure 4). As such, we treated C8PA cells with varying concentrations of **1** and determined the effect on interaction of AFABP/aP2 with HSL (Figure 4). The lower concentration of **1**, 1 μM, decreased basal FRET, but was ineffective in altering forskolin-stimulated FRET (data not shown). Cells treated with 10 μM **1** exhibited reduced FRET, both under basal and forskolin stimulated conditions. These results demonstrate that **1** functions as an antagonist of the protein-protein interaction of AFABP/aP2 with HSL.

### 1 effects in adipocytes and macrophages

Our previous studies and those of others have determined that targeted deletion of AFABP/aP2 decreases lipolysis in adipocytes[7-9]. Thus we repeated these experiments in 3T3L1 adipocytes to assess whether **1** would modulate the levels of lipolysis. The results show that the efflux of fatty acids was reduced in both basal and forskolin stimulated adipocytes (Figure 5). These results are again consistent with **1** functioning as an antagonist of AFABP/aP2 in cultured adipocytes.

Through the study of macrophages deficient in AFABP/aP2, we have previously demonstrated that inflammatory cytokine production is reduced[10]. To determine if **1** mimicked the null phenotype in macrophages, we pre-treated wild type macrophage cells with **1** and quantified

the production of IL-6, TNFα and MCP-1/CCL2 in response to LPS stimulation. For each of these targets, LPS stimulated a robust increase in expression and secretion of the inflammatory cytokines. **1** significantly reduced the LPS stimulated release of all three inflammatory cytokines measured (Figure 6), similar to the AFABP/aP2 knockout macrophages[10]. These results are consistent with **1** acting in macrophages as an antagonist of AFABP/aP2 function.

### 1 does not directly activate PPARγ

The AFABP/aP2 knockout mouse exhibits an overall phenotype of a reduced inflammatory state that has been suggested, at least in part, to arise from an increase in PPARγ activity. Since PPARγ and AFABP/aP2 both bind to hydrophobic ligands and have an overlapping set of molecules capable of binding in their respective cavities, we considered the possibility that **1** was directly activating PPARγ. Therefore we measured the expression of PPARγ targets, CD36 and Cpt1α in macrophages treated with **1** (Figure 7A). Whereas the known PPARγ ligand, 15-deoxy-delta12,14-prostaglandin J2, was proficient in elevating the mRNA levels of CD36 and Cpt1α, **1** treatment was not. Furthermore, we tested the ability of **1** to activate PPARγ in a heterologous luciferase reporter system in CV-1 cells (Figure 7B). While the thiazolidinedione, troglitazone activated a PPARγluciferase reporter, **1** did not activate the PPARγ reporter even at concentrations as high as 25 μM. These results indicate that **1** is not capable of direct activation of PPARγ.

## Discussion

AFABP/aP2 is an intracellular fatty acid carrier protein implicated in fatty acid metabolism through its ability to solubilize and traffic fatty acids. Various studies utilizing AFABP/aP2 null mice have established an important role for AFABP/aP2 in insulin sensitivity and overall metabolic homeostasis. More recently AFABP/aP2 has been shown to function as a fatty acid sensor, responding to the levels of free fatty acids by affecting target protein function via direct protein-protein interactions. Herein, we described the screening and identification of a small molecule inhibitor of AFABP/aP2. Through the displacement of the fluorescent molecule 1,8-ANS we demonstrated that AFABP/aP2 binds **1** with an affinity similar to fatty acids and thus it would be capable of functionally competing for binding in the ligand-binding cavity of AFABP/aP2. Furthermore, **1** treatment of adipocytes and macrophages produced phenotypes that mimicked those observed in AFABP/aP2 null cells/animals. In this study, the adipocytes and macrophages not only express AFABP/aP2, but also EFABP and HFABP. Although we found that the affinity of EFABP and HFABP for **1** was approximately 5 to 15-fold lower than for AFABP/aP2, it is unclear in these experiments whether binding of **1** to these other FABPs contributed to the anti-inflammatory phenotypes observed.

Improvements in the affinity of AFABP/aP2 for **1** could be realized by mutational engineering. Mutation of Y19 and/or F16 to arginine could stabilize the carbonyl oxygen of the ester group in **1** by functioning as a hydrogen bond donor. It may also be possible to stabilize the proximal thiofuran ring by mutating V25 to asparagine where the side chain amide nitrogen could potentially form an interaction to stabilize the thioether. An alternate approach would be to chemically modify **1** in order to increase affinity. We speculate that adding a carboxyl group to the distal thiofuran ring could increase the affinity by forming an interaction to the hydroxyl group of S55. Alternatively, exchanging the sulfur atom of the distal ring with a secondary amine could allow for an interaction with the main chain carbonyl of A75. Future experiments will be focused on design improvements in order to develop AFABP/aP2-specific inhibitor with higher affinity and selectivity.

The crystal structure of AFABP/aP2 with bound **1** showed it located in the ligand-binding cavity with the carboxyl group coordinated through R126 and Y128 in a manner similar to the way in which fatty acids are bound. There were no obvious large structural changes in this

high-resolution structure as compared to previous structures. This lack of structural change has been seen in apo structures as well as in several ligand-containing FABP structures. With this in mind, it remains a conundrum as to how the functional differences of holo-AFABP/aP2 are effectively communicated to other cellular proteins or processes. For example, it has been clearly demonstrated that holo-AFABP/aP2 efficiently forms protein-protein interactions with HSL and Jak2, as demonstrated through the lack of interaction of these target proteins with a non-fatty acid binding mutant of AFABP/aP2, R126Q. Thus a mechanism allowing recognition of holo-AFABP/aP2 must exist. Interestingly, **1** inhibits the interaction of AFABP/aP2 with HSL. It is not known if only exogenous ligands, such as **1**, or whether endogenous ligands exist that may also inhibit this protein-protein interaction.

In an attempt to identify the structural alterations that occur when an inhibitor (**1**) was bound, we analyzed regions of the protein that experience the largest difference upon binding. The four charged residues in the helix-turn-helix motif referred to as the charge quartet undergo small changes upon ligand binding. Even though the distance between the D17-R30 ion pair is slightly decreased with **1** bound to AFABP/aP2 compared to the apo protein, the distance between the second ion pair, D18-K21 is increased (0.77 Å). Since this domain is involved in interaction with HSL (and potentially other proteins), the increase may destabilize the motif and affect binding to interaction partners. However, a similar increase in the D18-K21 ion pair distance is also observed in the structure of the activating ligand, troglitazone, making it unlikely that this feature by itself is responsible for the inhibitory effects of **1**.

The fact that F57 can adopt an opened or closed conformation makes it an interesting candidate as a switch indicating that a specific ligand is bound in the ligand-binding cavity. This shift could, however, merely be a secondary effect due to steric hindrance between the bound ligand and the side chain of F57. As seen in Figure 2B, the ligands oleic acid and **1**, which both give rise to a open conformation of F57, extend out of the ligand-binding pocket and hence would occupy the same space as the side chain of F57 in its closed orientation. On the other hand, F57 is in its closed orientation when linoleic acid is bound. Linoleic acid adopts a bent conformation in the cavity and therefore doesn't extend as far out of the cavity as do oleic acid or **1**. It is plausible that a closed conformation of F57 is the most energetically favorable and therefore the preferred orientation when possible.

The A36-K37 peptide flip observed in some structures while absent in others is also an interesting feature (Figure 2D). Residues A36 and K37 are located in a disordered region connecting α-helix 2 with β-strand B. In the apo form of AFABP/aP2, the carbonyl group of A36 does not form any interactions with other residues or solvent molecules. In **1**, as well as AFABP/aP2 with oleic acid, the carbonyl group of A36 is rotated almost 180° and can form a hydrogen bond to a water molecule positioned 3 Å away. Furthermore, this water forms three other hydrogen bonds, one with the carbonyl group of A33, one with the guanidinium group of R126 and one with another water molecule. This water molecule network can be extended from the A36 carbonyl group throughout a large portion of the ligand-binding cavity. The water molecule in proximity to the carbonyl group of A36 is also present in the apo structure of AFABP/aP2 although it cannot form a hydrogen bond with this residue since it is facing the other direction. It is also shifted so it is positioned almost 0.5 Å farther away from R126. In addition, the structure of the apo form contains fewer water molecules so the hydrogen-bonding network extending into the ligand-binding pocket cannot be traced. One possibility is that a peptide rotation at A36 and K37 confers more stability to R126, which interacts directly with different ligands. Unfortunately, this alone cannot explain the differences specific ligands exert on the function of the protein, since only some ligands induce this peptide flip.

The phenotypes demonstrated in this paper are consistent with **1** acting as an antagonist of AFABP/aP2, since the effects mimicked those seen in the AFABP/aP2 knockout mice.

Additionally, since PPARγ activation would mimic many of the observed phenotypes associated with reduced inflammatory states, we tested the direct and/or indirect modes of **1** activation of PPARγ. In both cases, **1** was incapable of demonstrating PPARγ activation. However, it is also possible that **1** can bind and/or affect other cellular targets as well. One model proposed to explain the differences detected in AFABP/aP2 null macrophages involves the indirect action of unbound fatty acids. These fatty acids could activate PPARγ resulting in increased target gene expression and inhibition of inflammatory cytokine production. The data included here do not support this model. While inflammatory cytokine production was decreased, expression of PPARγ targets was not increased. Thus an alternative model that includes alteration of PPARγ activity through protein-protein interaction of AFABP/aP2, may at least partially explain the changes detected. Further work is necessary to evaluate this model.

## Experimental Section

### Purification and ligand-binding analysis

*Escherichia coli* BL21 (DE3) cells, transformed with a gene encoding His-tagged AFABP/aP2 (or other FABPs), were grown in rich media and 1 mM IPTG was added for four hours to induce protein expression. The cells were harvested by centrifugation and lysed in a French press. The debris was pelleted by centrifugation at 100,000×g for 60 minutes and the solubilized protein purified using a nickel affinity chromatography. The pooled eluate was subjected to lipidex-1000 chromatography to remove any endogenously bound ligands and dialyzed into 25 mM Tris-HCl (pH 7.4), 50 mM NaCl plus 5% glycerol for storage at -80 °C. The purity of the isolated FABPs was verified by SDS-PAGE.

To analyze the ligand binding properties of the FABPs, the fluorescent ligand 1-anilinonapthalene 8-sulfonic acid (1,8-ANS) was utilized as described by Kane and Bernlohr[21]. Briefly, 1,8 ANS was dissolved in absolute ethanol and diluted with 25 mM Tris-HCl (pH 7.4) to a final concentration of 5 μM (final EtOH concentration of 0.05%). Protein was titrated into 500 μL 1,8-ANS and the fluorescence enhancement was measured using a Perkin Elmer 650-10S fluorescence spectrophotometer with 4 nm excitation and emission slit widths. Quantitative analysis of ligand binding was evaluated using non-linear regression using PRISM software.

### Small molecule library screening

A Maybridge chemical library (≥ 90-95% purity; Fisher Scientific International) was screened for compounds binding to AFABP/aP2 using a Biomek FX workstation integrated into a Saigen core system and a molecular devices Gemini XPS plate reader. Each well contained 12 μM AFABP/aP2 complexed with 400 nM 1-anilinonapthalene 8-sulfonic acid and the fluorescence reduction due to displacement of the bound fluorophore by the test compounds measured in duplicate. Each plate also contained a positive control (oleic acid) as well as a negative control (methyl octanoate) as internal standards and controls.

### X-ray crystallography

Non His-tagged AFABP/aP2 was purified as described previously with minor modifications[24]. Briefly, AFABP/aP2 was expressed in *E. coli*, harvested by centrifugation, and the cells lysed with French Press. After centrifugation of the crude extract, protamine sulfate (5% final w/v) was added to the supernatant followed by centrifugation. The pH of the protamine sulfate soluble protein was adjusted to 5 and proteins allowed to precipitate overnight at 4 °C. After centrifugation and neutralization, the sample was chromatographed through a Lipidex-1000 column followed by two rounds of gel filtration using Superdex G75 resin. The fractions containing AFABP/aP2 were pooled and applied to a long-chain fatty acid affinity column[36] to obtain pure AFABP/aP2, which was verified by SDS-PAGE. The purified

AFABP/aP2 was concentrated to 10 mg/ml, dialyzed against 12.5 mM Hepes (pH 7.5), 1 mM DTT, and incubated over night with 4-fold molar excess of **1** (dissolved in DMSO; 1% final DMSO concentration) at room temperature while stirring.

The sitting drop method (1.3-3.1 M sodium/potassium phosphate; pH 6.8-7.6) was used to obtain crystals[25]. The plates were incubated at 18 °C and rod shaped crystals grew within five days with the best crystal found in a well containing 2.5 M sodium/potassium phosphate (pH 7.0). Crystals were flash frozen in liquid nitrogen with 20% glycerol in the mother liquor and stored until data collection. Diffraction data was collected from a single crystal using a Rigaku MicroMax 007HF generator with a Cu anode and a Rigaku Raxis IV++ detector and was processed using the HKL2000 software[37]. The space group was determined to be $C222_1$. Molecular replacement using the previously solved apo form (PDB ID 1LIB) of the protein was conducted with MolRep[38] in the CCP4 package[39] and the refinement was performed using Refmac540 and WinCoot[41]. The electron density in the $F_o$-$F_c$ map clearly indicated the orientation and position of the **1** ligand in the cavity of AFABP. Data collection and refinement statistics are shown in Table 2.

## Fluorescence Resonance Energy Transfer

C8PA lipocytes used for FRET analysis were cultured as described previously[16, 35]. C8PA cells were grown on polylysine-coated 13-mm coverslips and transfected with pECFP-HSL and/or pEYFP-AFABP expression plasmids. After 24 hours, the cells were lipid-loaded with 300 μM oleic acid, 100 μM bovine serum albumin for 24 h followed by treatment of 1 or 10 μM of **1** complexed with 100 μM bovine serum albumin for an additional 24 hours. Lipolytic conditions were initiated by the addition of 20 μM forskolin and digital images captured between two and four hours later. During microscopy, cells were kept in medium at 37 °C with 5% $CO_2$ until imaging at room temperature. Images were captured and real-time FRET measurements were performed as previously reported[16, 35]. Normalized FRET (NFRET) was calculated from 15-20 cells as previously reported[31].

## Adipocyte lipolysis

Adipocytes were differentiated from confluent 3T3-L1 preadipocytes by the addition of methylisobutylxanthine, dexamethasone and insulin for two days, insulin for an additional two days and maintained in DMEM plus 10% FBS[42]. After eight days, the adipocytes were incubated in Krebs Ringer Hepes with 2% BSA for 60 minutes in the presence or absence of 20 μM forskolin. Total NEFA secreted was quantified by the NEFA quantification kit (Wako).

## Macrophage growth and treatments

Bone marrow-derived macrophages were isolated from FABP+/+ C57Bl/6J animals and plated at $10^5$ cells per well in 96-well plates (Nalge-Nunc International, Rochester, NY). Cells were pre-incubated with the indicated concentrations of **1** or carrier (DMSO) for 48 hours. Additionally, cells were left untreated or stimulated with the indicated concentrations of LPS (Sigma-Aldrich) for 24 h. Supernatants were harvested and assayed by ELISA for IL-6, MCP-1/CCL2, and TNFα (BD Biosciences-OptEIA).

## Real-time PCR

Wild-type bone marrow-derived macrophages were plated at $2\times10^6$ cells/well in 6-well plates (Corning) and stimulated with 5 μM $15dPGJ_2$ (BIOMOL) overnight following 48 hours pre-incubation with **1**. mRNA was isolated and cDNA synthesized using μMACS One-Step cDNA columns (Miltenyi Biotech). Real-time PCR was performed on a DNA Opticon 2 Monitor (MJ Research, currently BioRad) using SYBR Green (New England Biolabs). CD36 and carnitine palmitoyltransferase 1A (Cpt1a) were analyzed by Quantitect Primer Assays (Qiagen). β-actin

was used as the reference gene with primers purchased from Clontech (Mountain View, CA). Relative mRNA expression was quantified using the relative expression software tool.

### Reporter assays

CV-1 cells were maintained in DMEM with 10% fetal bovine serum at 37 °C. Transient transfections were performed using lipofectamine 2000 as per the manufacturer's directions (Invitrogen). Co-transfected were pCMV expression plasmids for PPARγ and RXRα and an AFABP/aP2 promoter-luciferase reporter plasmid. All transfections were normalized to the expression of a co-transfected pCMV-renilla luciferase plasmid. Cells were treated 18 hours after transfection with varying concentrations of ligand and after another 24 hours were washed, harvested and luciferase activity assayed using the Dual Luciferase Reporter Assay System (Promega, Madison, WI).

## Acknowledgments

We would like to thank the members of the Bernlohr laboratory for helpful comments and suggestions during the preparation of this manuscript. We would also like to thank Ed Hoeffner for technical assistance in crystallography and Nick Hahn of the University of Minnesota Biotechnology Institute for library screening. This research was supported by a Minnesota Partnership for Biotechnology and Medical Genomics Grant SPAP-05-0013-P-FY06 and the computational resources were provided by the Basic Sciences Computing Laboratory of the University of Minnesota Supercomputing Institute. This work was supported by NIH DK053189 to DAB, the Minnesota Obesity Center (DK050456) and NIH AI048850 to JS.

## References

1. Storch J, Corsico B. The emerging functions and mechanisms of mammalian fatty acid-binding proteins. Annu Rev Nutr 2008;28:73–95. [PubMed: 18435590]
2. Hotamisligil GS. Inflammation and endoplasmic reticulum stress in obesity and diabetes. Int J Obes (Lond) 2008;32:S52–54. [PubMed: 19136991]
3. Furuhashi M, Fucho R, Gorgun CZ, Tuncman G, Cao H, Hotamisligil GS. Adipocyte/macrophage fatty acid-binding proteins contribute to metabolic deterioration through actions in both macrophages and adipocytes in mice. J Clin Invest 2008;118:2640–2650. [PubMed: 18551191]
4. Makowski L, Boord JB, Maeda K, Babaev VR, Uysal KT, Morgan MA, Parker RA, Suttles J, Fazio S, Hotamisligil GS, Linton MF. Lack of macrophage fatty-acid-binding protein aP2 protects mice deficient in apolipoprotein E against atherosclerosis. Nat Med 2001;7:699–705. [PubMed: 11385507]
5. Hotamisligil GS, Johnson RS, Distel RJ, Ellis R, Papaioannou VE, Spiegelman BM. Uncoupling of obesity from insulin resistance through a targeted mutation in aP2, the adipocyte fatty acid binding protein. Science 1996;274:1377–1379. [PubMed: 8910278]
6. Shum BO, Mackay CR, Gorgun CZ, Frost MJ, Kumar RK, Hotamisligil GS, Rolph MS. The adipocyte fatty acid-binding protein aP2 is required in allergic airway inflammation. J Clin Invest 2006;116:2183–2192. [PubMed: 16841093]
7. Coe NR, Simpson MA, Bernlohr DA. Targeted disruption of the adipocyte lipid-binding protein (aP2 protein) gene impairs fat cell lipolysis and increases cellular fatty acid levels. J Lipid Res 1999;40:967–972. [PubMed: 10224167]
8. Baar RA, Dingfelder CS, Smith LA, Bernlohr DA, Wu C, Lange AJ, Parks EJ. Investigation of in vivo fatty acid metabolism in AFABP/aP2$^{-/-}$ mice. Am J Physiol Endocrinol Metab 2005;288:E187–193. [PubMed: 15367400]
9. Scheja L, Makowski L, Uysal KT, Wiesbrock SM, Shimshek DR, Meyers DS, Morgan M, Parker RA, Hotamisligil GS. Altered insulin secretion associated with reduced lipolytic efficiency in aP2-/- mice. Diabetes 1999;48:1987–1994. [PubMed: 10512363]
10. Makowski L, Brittingham KC, Reynolds JM, Suttles J, Hotamisligil GS. The fatty acid-binding protein, aP2, coordinates macrophage cholesterol trafficking and inflammatory activity. Macrophage expression of aP2 impacts peroxisome proliferator-activated receptor gamma and IkappaB kinase activities. J Biol Chem 2005;280:12888–12895. [PubMed: 15684432]

11. LaLonde JM, Bernlohr DA, Banaszak LJ. The up-and-down beta-barrel proteins. Faseb J 1994;8:1240–1247. [PubMed: 8001736]
12. Zimmerman AW, Veerkamp JH. New insights into the structure and function of fatty acid-binding proteins. Cell Mol Life Sci 2002;59:1096–1116. [PubMed: 12222958]
13. Chmurzynska A. The multigene family of fatty acid-binding proteins (FABPs): function, structure and polymorphism. J Appl Genet 2006;47:39–48. [PubMed: 16424607]
14. Richieri GV, Ogata RT, Zimmerman AW, Veerkamp JH, Kleinfeld AM. Fatty acid binding proteins from different tissues show distinct patterns of fatty acid interactions. Biochemistry 2000;39:7197–7204. [PubMed: 10852718]
15. Jenkins-Kruchten AE, Bennaars-Eiden A, Ross JR, Shen WJ, Kraemer FB, Bernlohr DA. Fatty acid-binding protein-hormone-sensitive lipase interaction. Fatty acid dependence on binding. J Biol Chem 2003;278:47636–47643. [PubMed: 13129924]
16. Smith AJ, Thompson BR, Sanders MA, Bernlohr DA. Interaction of the adipocyte fatty acid-binding protein with the hormone-sensitive lipase: regulation by fatty acids and phosphorylation. J Biol Chem 2007;282:32424–32432. [PubMed: 17785468]
17. Thompson BR, Muzurkiewicz-Munoz AM, Suttles J, Carter-Su C, Bernlohr DA. Interaction of Adipocyte Fatty Acid Binding Protein and JAK2: AFABP/aP2 as a Regulator of JAK2 Signaling. J Biol Chem. 2009
18. Adida A, Spener F. Adipocyte-type fatty acid-binding protein as inter-compartmental shuttle for peroxisome proliferator activated receptor gamma agonists in cultured cell. Biochim Biophys Acta 2006;1761:172–181. [PubMed: 16574478]
19. Ayers SD, Nedrow KL, Gillilan RE, Noy N. Continuous nucleocytoplasmic shuttling underlies transcriptional activation of PPARgamma by FABP4. Biochemistry 2007;46:6744–6752. [PubMed: 17516629]
20. Hertzel AV, Smith LA, Berg AH, Cline GW, Shulman GI, Scherer PE, Bernlohr DA. Lipid metabolism and adipokine levels in fatty acid-binding protein null and transgenic mice. Am J Physiol Endocrinol Metab 2006;290:E814–823. [PubMed: 16303844]
21. Kane CD, Bernlohr DA. A simple assay for intracellular lipid-binding proteins using displacement of 1-anilinonaphthalene 8-sulfonic acid. Anal Biochem 1996;233:197–204. [PubMed: 8789718]
22. Xu Z, Bernlohr DA, Banaszak LJ. Crystal structure of recombinant murine adipocyte lipid-binding protein. Biochemistry 1992;31:3484–3492. [PubMed: 1554730]
23. Xu Z, Bernlohr DA, Banaszak LJ. The adipocyte lipid-binding protein at 1.6-A resolution. Crystal structures of the apoprotein and with bound saturated and unsaturated fatty acids. J Biol Chem 1993;268:7874–7884. [PubMed: 8463311]
24. Xu ZH, Buelt MK, Banaszak LJ, Bernlohr DA. Expression, purification, and crystallization of the adipocyte lipid binding protein. J Biol Chem 1991;266:14367–14370. [PubMed: 1650358]
25. LaLonde JM, Bernlohr DA, Banaszak LJ. X-ray crystallographic structures of adipocyte lipid-binding protein complexed with palmitate and hexadecanesulfonic acid. Properties of cavity binding sites. Biochemistry 1994;33:4885–4895. [PubMed: 8161548]
26. LaLonde JM, Levenson MA, Roe JJ, Bernlohr DA, Banaszak LJ. Adipocyte lipid-binding protein complexed with arachidonic acid. Titration calorimetry and X-ray crystallographic studies. J Biol Chem 1994;269:25339–25347. [PubMed: 7929228]
27. Gillilan RE, Ayers SD, Noy N. Structural basis for activation of fatty acid-binding protein 4. J Mol Biol 2007;372:1246–1260. [PubMed: 17761196]
28. Dundas J, Ouyang Z, Tseng J, Binkowski A, Turpaz Y, Liang J. CASTp: computed atlas of surface topography of proteins with structural and topographical mapping of functionally annotated residues. Nucleic Acids Res 2006;34:W116–118. [PubMed: 16844972]
29. Simpson MA, Bernlohr DA. Analysis of a series of phenylalanine 57 mutants of the adipocyte lipid-binding protein. Biochemistry 1998;37:10980–10986. [PubMed: 9692991]
30. Jenkins AE, Hockenberry JA, Nguyen T, Bernlohr DA. Testing of the portal hypothesis: analysis of a V32G, F57G, K58G mutant of the fatty acid binding protein of the murine adipocyte. Biochemistry 2002;41:2022–2027. [PubMed: 11827549]
31. Smith AJ, Sanders MA, Juhlmann BE, Hertzel AV, Bernlohr DA. Mapping of the hormone-sensitive lipase binding site on the adipocyte fatty acid-binding protein (AFABP). Identification of the charge

quartet on the AFABP/aP2 helix-turn-helix domain. J Biol Chem 2008;283:33536–33543. [PubMed: 18820256]

32. Sali A, Blundell TL. Comparative protein modelling by satisfaction of spatial restraints. J Mol Biol 1993;234:779–815. [PubMed: 8254673]
33. Shen WJ, Liang Y, Hong R, Patel S, Natu V, Sridhar K, Jenkins A, Bernlohr DA, Kraemer FB. Characterization of the functional interaction of adipocyte lipid-binding protein with hormone-sensitive lipase. J Biol Chem 2001;276:49443–49448. [PubMed: 11682468]
34. Shen WJ, Sridhar K, Bernlohr DA, Kraemer FB. Interaction of rat hormone-sensitive lipase with adipocyte lipid-binding protein. Proc Natl Acad Sci U S A 1999;96:5528–5532. [PubMed: 10318917]
35. Smith AJ, Sanders MA, Thompson BR, Londos C, Kraemer FB, Bernlohr DA. Physical association between the adipocyte fatty acid-binding protein and hormone-sensitive lipase: a fluorescence resonance energy transfer analysis. J Biol Chem 2004;279:52399–52405. [PubMed: 15456755]
36. Buelt MK, Xu Z, Banaszak LJ, Bernlohr DA. Structural and functional characterization of the phosphorylated adipocyte lipid-binding protein (pp15). Biochemistry 1992;31:3493–3499. [PubMed: 1372828]
37. Otwinowski, Z.; Minor, W. Processing of X-ray Diffraction Data Collected in Oscillation Mode. In: Carter, C.; Sweet, R., editors. Methods in Enzymology, Macromolecular Crystallography, part A. Academic Press; New York: 1997.
38. Vagin A, Teplyakov A. MOLREP: an Automated Program for Molecular Replacement. J Appl Cryst 1997;30:1022–1025.
39. The CCP4 suite: programs for protein crystallography. Acta Crystallogr D Biol Crystallogr 1994;50:760–763. [PubMed: 15299374]
40. Murshudov GN, Vagin AA, Dodson EJ. Refinement of macromolecular structures by the maximum-likelihood method. Acta Crystallogr D Biol Crystallogr 1997;53:240–255. [PubMed: 15299926]
41. Emsley P, Cowtan K. Coot: model-building tools for molecular graphics. Acta Crystallogr D Biol Crystallogr 2004;60:2126–2132. [PubMed: 15572765]
42. Student AK, Hsu RY, Lane MD. Induction of fatty acid synthetase synthesis in differentiating 3T3-L1 preadipocytes. J Biol Chem 1980;255:4745–4750. [PubMed: 7372608]
43. DeLano, WL. The PyMol Molecular Graphics System. Palo Alto, CA, USA: 2002.

## Abbreviations

**AFABP/aP2**
adipocyte fatty acid binding protein

**1,8-ANS**
1-anilinonapthalene 8-sulfonic acid

**Cpt1a**
carnitine palmitoyltransferase 1A

**EFABP**
epithelial fatty acid binding protein

**FABP**
fatty acid binding protein

**FRET**
fluorescence resonance energy transfer

**HFABP**
heart fatty acid binding protein

**HSL**
hormone sensitive lipase

**IFABP**
: intestinal fatty acid binding protein

**LFABP**
: liver fatty acid binding protein

**PPARγ**
: peroxisome proliferator activated receptor γ

**1**
: Maybridge HTS01037

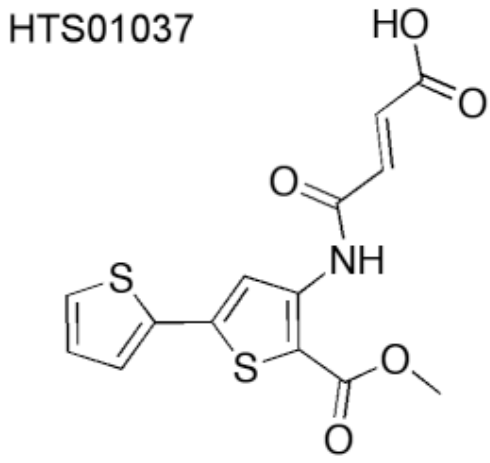


4-{[2-(methoxycarbonyl)-5-(2-thienyl)-3-thienyl]amino}-4-oxo-2-butenoic acid

**Figure 1. Chemical structure of 1**

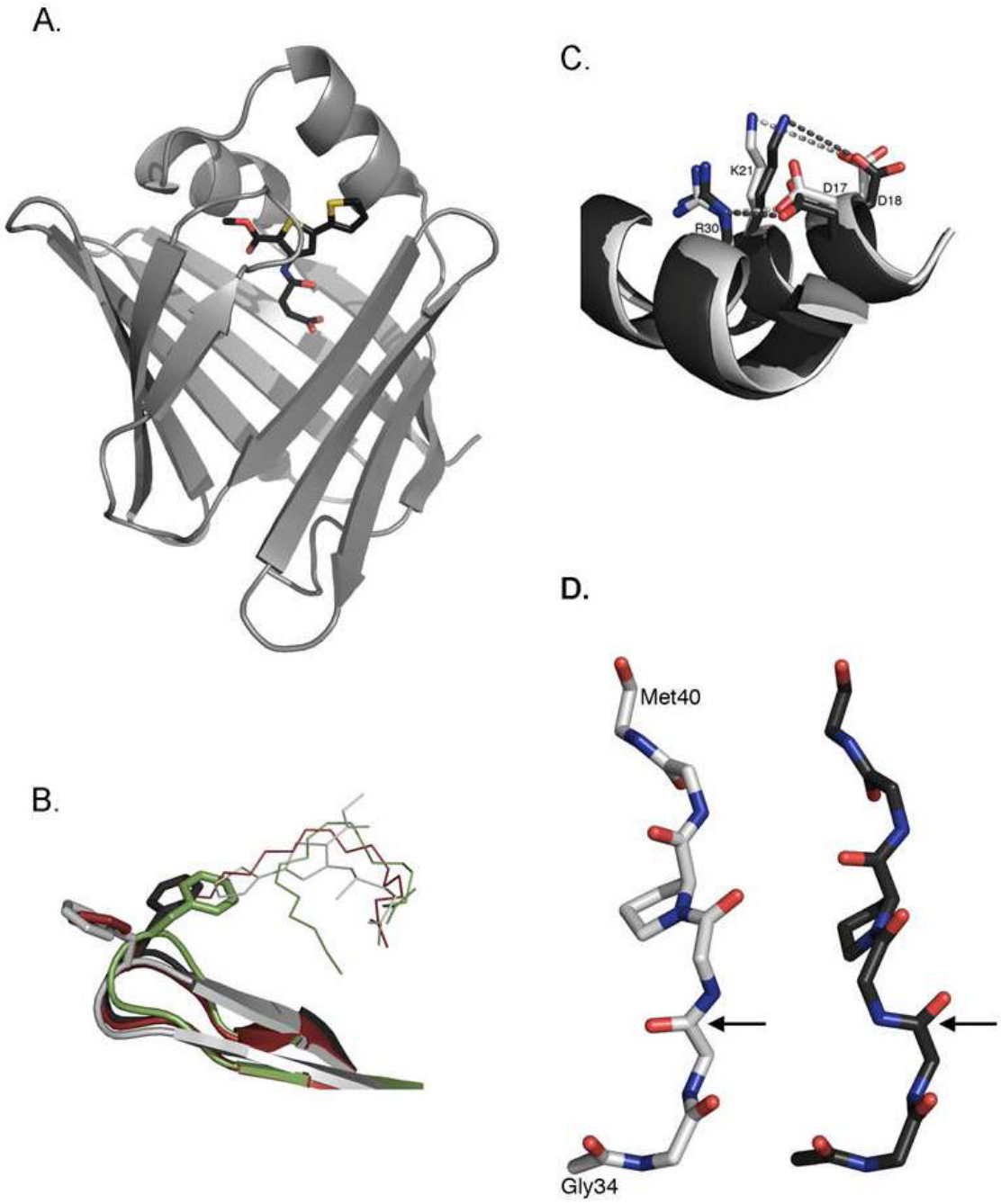


**Figure 2. Structure of AFABP/aP2 complexed with 1**

A. Ribbon representation of the crystal structure of AFABP/aP2 with **1** highlighted in black and shown in sticks in the ligand-binding cavity. B. The side chain of Phe57 from different structures are aligned and represented as sticks. AFABP/aP2 with **1** is shown in light gray, apo AFABP/aP2 (PDB ID 1LIB) in black, AFABP/aP2 with linoleic acid (PDB ID 2Q9S) in green and AFABP/aP2 with oleic acid (PDB ID 1LID) in brown. Ligands are represented as lines and are color coded as mentioned above. C. The helical domain is shown in cartoon representation and residues in the charge quartet are represented as sticks. AFABP/aP2 with **1** is shown in light gray and apo AFABP/aP2 in black. Distances between the ion pairs are represented as dashed lines and color coded as the proteins. D. The peptide flip between alanine

36 and lysine 37 are shown. AFABP/aP2 with **1** is shown in light gray, apo AFABP/aP2 in black. Arrow points to the main chain carbonyl of alanine 36. Figure was prepared using the program PyMol[43].

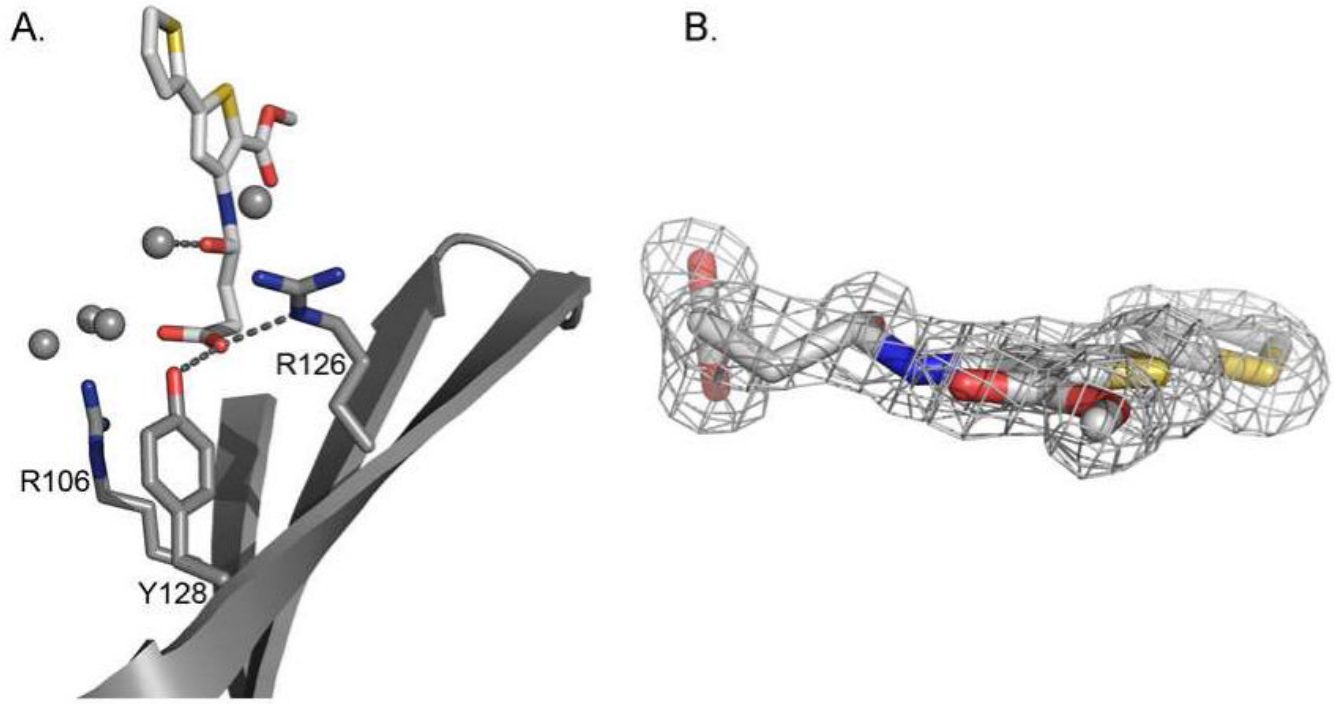


**Figure 3. Structure of 1 bound to AFABP/aP2**

A. Coordination of **1** in AFABP/aP2. Residues previously implicated in coordination of fatty acids are shown in sticks. Waters are shown as gray balls and hydrogen bonds to **1** are represented as dashed lines. B. Electron density of **1** with the 2Fo-Fc map contoured at 1.5 σ. Figure was prepared using the program PyMol[43].

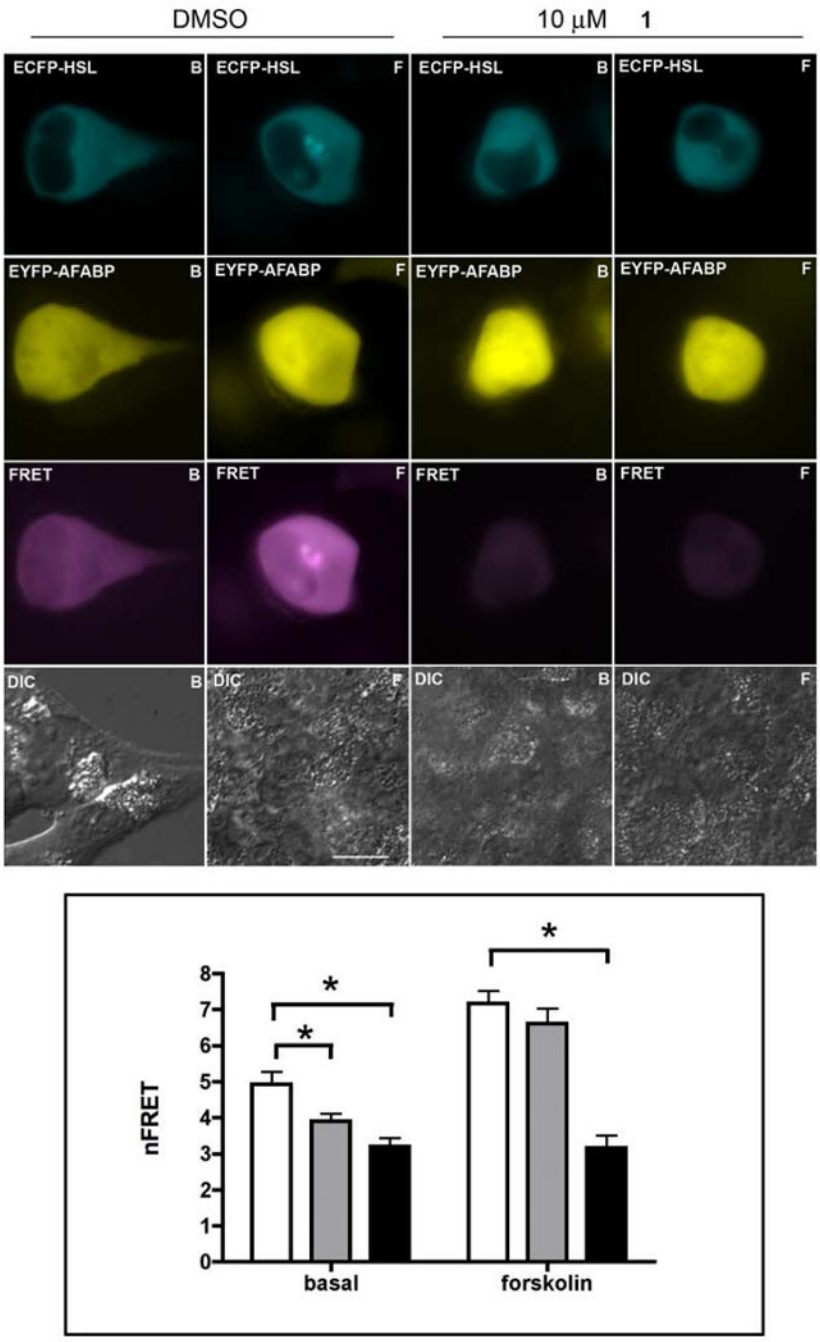


**Figure 4. 1 functions as an antagonist of the interaction of AFABP/aP2 with HSL**

A. Fluorescence resonance energy transfer (colored magenta) between ECFP-HSL and EYFP-AFABP/aP2 in C8PA cells under basal (B) and forskolin (F) stimulation. The cells were treated either with DMSO or 10 μM **1**. The scale bar represents 5 μm. B. NFRET was calculated as described under "Experimental Section". White bars, DMSO; gray bars, 1 μM **1**; black bars, 10 μM **1**. Error bars represent standard error of the mean (n=15). The * denotes statistical significance ($p<0.05$) as compared to the DMSO treated.

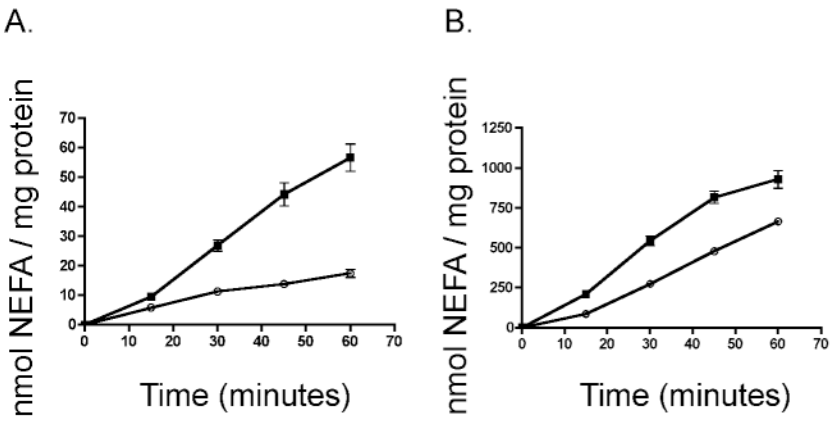


**Figure 5. Treatment of 3T3L1 adipocytes with 1 inhibits lipolysis**

3T3L1 adipocytes were treated with DMSO (closed squares) or **1** (open circles) for 24 hours. Aliquots of medium were taken and non-esterified fatty acids were quantified at various times and normalized to mg protein. A. Basal lipolysis. B. Forskolin-stimulated lipolysis.

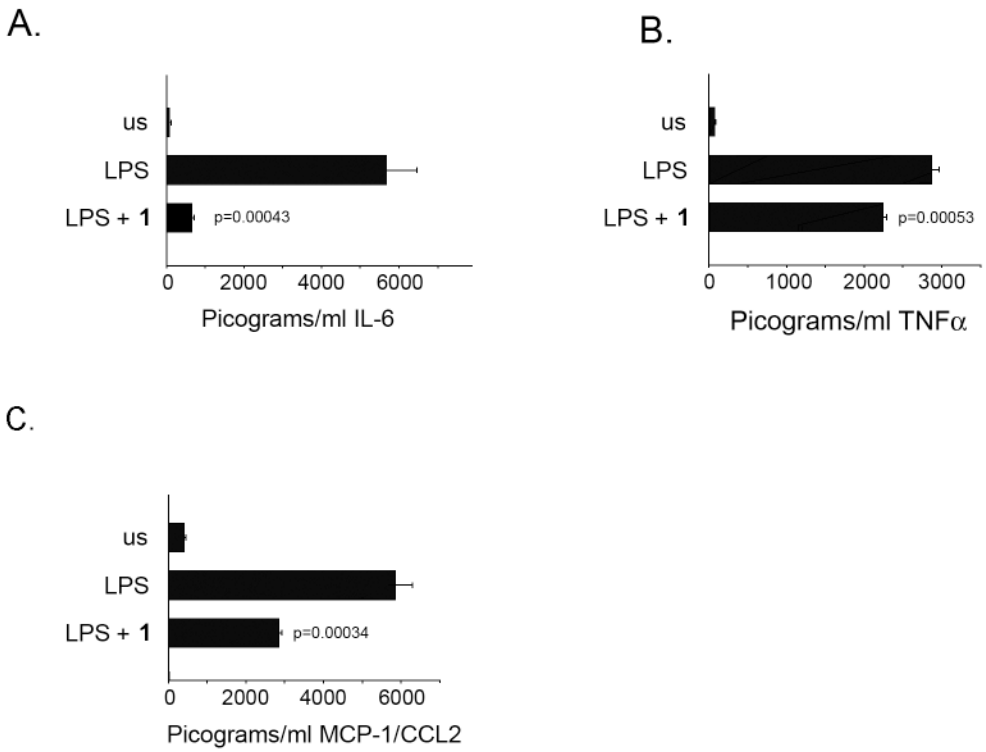


**Figure 6. Treatment of macrophages with 1 inhibits inflammatory cytokine production**

Bone marrow-derived macrophages were cultured and pre-treated with or without **1**, followed by LPS stimulation. Cytokine production was quantified by ELISA. A. IL-6. B. TNFα. C. MCP-1. p values < 0.05 were considered significant. us denotes no LPS stimulation.

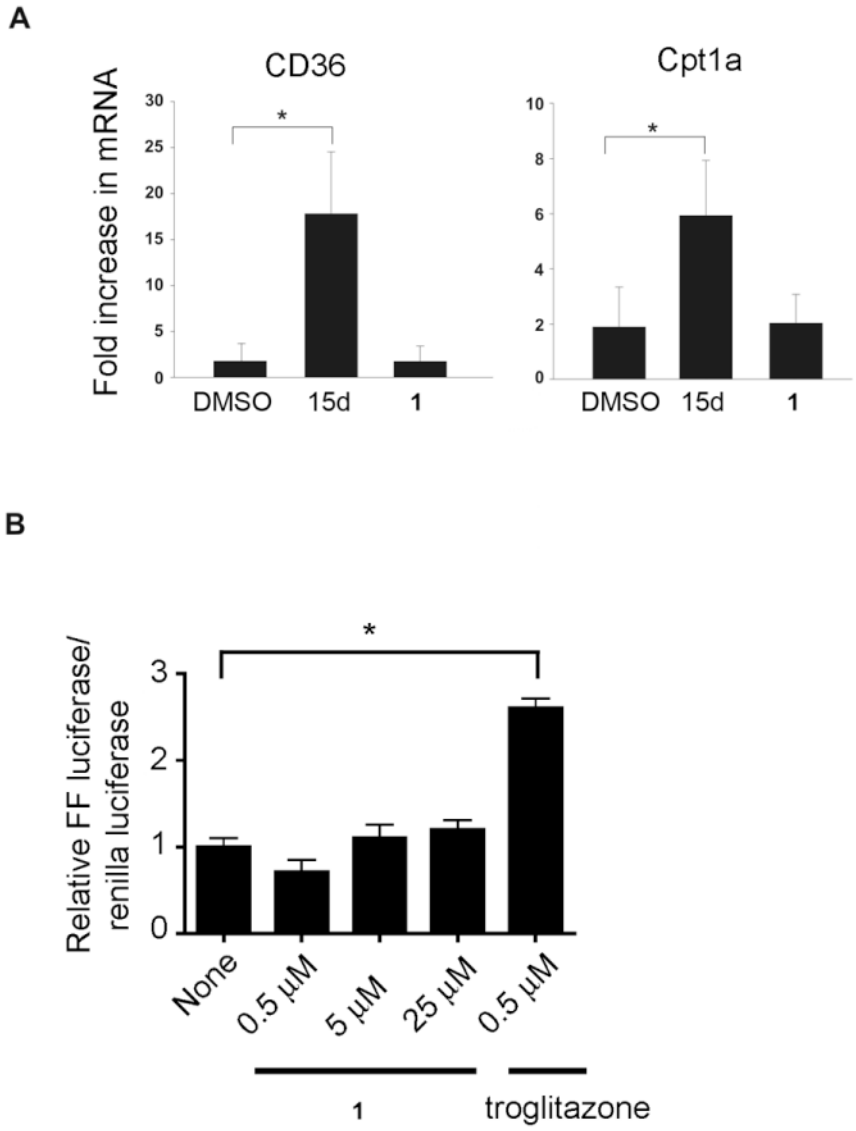


**Figure 7. 1 does not activate PPARγ in macrophages or CV-1 cells**

A. The expression of the PPARγ-regulated genes CD36 and Cpt1a was analyzed by real-time PCR in response to 5 μM 15dPGJ$_2$ or 500 nM **1,** referred to as HTS (DMSO as control). Fold increase in mRNA was quantified using β-actin as a reference gene and an un-stimulated sample as the baseline for expression using the relative expression tool. B. PPARγ activation was measured in CV-1 cells using a luciferase reporter assay. Cells were exposed to increasing amounts of **1**. Troglitazone was used as a positive control. * P value <0.05 were considered significant.

**Table 1**

Binding of **1** to FABPs[a]

| Protein | Apparent Ki (μM) | P value |
|---|---|---|
| AFABP/aP2 | 0.67 +/- 0.18 | |
| EFABP | 3.40 +/- 0.60 | 0.04 |
| HFABP | 9.07 +/- 1.71 | 0.04 |
| IFABP | 6.57 +/- 1.55 | 0.06 |
| LFABP | 8.17 +/- 1.28 | 0.03 |

[a]The displacement of 1,8-ANS by **1** reported as the mean and standard error of the mean (n=3). P value relative to AFABP/aP2.

**Table 2**

Crystallographic Data Collection and Refinement Statistics[a]

| | |
|---|---|
| space group | $C222_1$ |
| cell parameters: *a, b, c* (Å) | 77.0, 94.1, 49.7 |
| resolution (Å) | 1.70 |
| <I>/σ<I> | 49.1 (6.5) |
| completeness (%) | 99.8 (98.4) |
| redundancy | 6.8 (6.5) |
| $R_{sym}$ (%)[b] | 3.5 (27.7) |
| unique reflections | 20158 |
| $R_{work}/R_{free}$ (%)[c] | 17.5/19.5 |
| No. of atoms | |
| protein/ligand/water | 1022/22/225 |
| Average B-factors (Å$^2$) | |
| protein/ligand/water | 17.2/16.6/33.5 |
| Rmsd bond length (Å) | 0.011 |
| Rmsd bond angles (°) | 1.855 |

[a] Data in parentheses are for the highest resolution bin.

[b] $R_{sym} = \Sigma| I_i - \langle I \rangle | / \Sigma I_i$, where $I_i$ indicates the intensity of the *i*th observation and $\langle I \rangle$ indicates the mean intensity of the reflection.

[c] $R_{work} = \Sigma|F_{obs} - F_{calcd}|/\Sigma F_{obs}$, where $F_{obs}$ and $F_{calcd}$ are the observed and calculated structure factors, respectively. $R_{free}$ were calculated using the same equation as for $R_{work}$ but using the reflections in the test set instead of the working set.